

SWITCHING NEURO-FUZZY CONTROL WITH ANTISATURATING LOGIC. EXPERIMENTAL RESULTS FOR HYDROSTATIC SERVOACTUATORS

Ioan URSU¹, George TECUCEANU¹, Adrian TOADER¹, Constantin CALINOIU²

¹INCAS-Elie Carafoli National Institute for Aerospace Research

²University “Politehnica” of Bucharest

e-mail: iursu@incas.ro

Continuing recent works of the authors, the paper shows the developing and the application of a neuro-fuzzy control law to the positioning loop of a hydrostatic type servoactuator. Experimental results are presented concerning dynamical behavior of the system by using this “intelligent” controller. Finally, arguments about the advantages of the new designed controller are summarized.

Key words: Pump controlled electrohydraulic servoactuator, Hydrostatic servoactuator, Mathematical model, Intelligent neuro-fuzzy switching control, Antisaturating fuzzy logic, Numerical simulation, Algorithm implementation, Experimental results.

1. INTRODUCTION

It is well known [1–8] that the pump controlled system keeps on the servovalve controlled ones [9–12] the advantages of a better linearity, stability and efficiency due to the eliminating of throttle losses at the valve. And, first of all, the pump controlled system avoids the requirement of a large central system with a reservoir. Thus, the pump controlled actuation is in fact a cost and weight effective actuation.

This work describes experimental tests performed on the positioning Hydrostatic ServoActuator (HSA) [6] having implemented a switching neuro-fuzzy control law with antisaturating logic. The organization of the work is as follow. In Section 2, the HSA physical and mathematical models and the control synthesis are shortly described. The Section 3 describes the experimental set up and presents experimental results on the system, underlining its dynamical performance essentially represented by the time constant. Section 4 is devoted to summarize some conclusions concerning the advantages of the intelligent controllers versus the classical ones.

2. MATHEMATICAL MODELING AND NEURO-FUZZY CONTROL SYNTHESIS

Consider the architecture of a pump controlled HSA physical model given in Fig. 1.

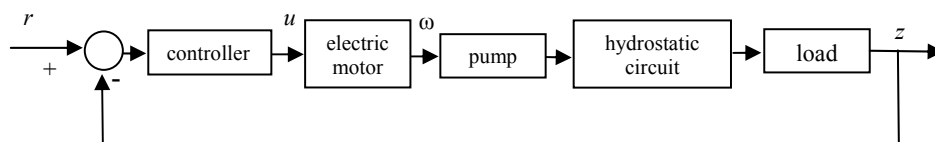


Fig. 1 – Architecture of the pump controlled HSA physical model.

The primary component of the HSA is a double cylinder with simple action supplied with hydraulic oil by a fixed displacement, bidirectional gear pump. The transmission of the fluid power is obtained by very stiffly coupling the pump to the hydraulic cylinder, thus the electrohydraulic servovalve is not required. The pump is driven by an AC electric motor. The system is of closed type, so there is no direct contact between the oil and air. The electric motor has as analog input a speed reference signal from the range of $\pm 5V$.

The rod position is controlled by varying the speed of the electric motor. The mathematical model of the HSA system is the following [4–8]

$$\begin{aligned}
 \dot{x}_1 &= x_2, \dot{x}_2 = \frac{1}{m}[-kx_1 - fx_2 - F_f + S(x_4 - x_5)], \\
 \dot{x}_3 &= x_2 - \frac{\sigma_0 |x_2| x_3}{F_c + (F_s - F_c)e^{-(x_2/v_s)^2}}, \quad F_f = \sigma_1 \dot{x}_3 + f_v x_2 + \sigma_0 x_3, \\
 \dot{x}_4 &= \frac{B}{V_{01} + Sx_1} [D_p x_6 - C_{ip}(x_4 - x_5) - C_{ep}(x_4 - p_r) - C_{ec} x_4 - Sx_2], \\
 \dot{x}_5 &= \frac{B}{V_{02} - Sx_1} [-D_p x_6 + C_{ip}(x_4 - x_5) - C_{ep}(x_5 - p_r) - C_{ec} x_5 + Sx_2], \\
 V_{01} &= V_{D1} + Sl; V_{02} = V_{D2} + Sl, \tau \dot{x}_6 + x_6 = k_m u.
 \end{aligned} \tag{1}$$

The system includes a LuGre model of dry friction F_f [8].

The state variables are: $x_1 \equiv z$ – load displacement [m]; x_2 – load velocity [m/s]; x_3 – state value concerning internal friction [m]; x_4 – pressure in cylinder chamber one [Pa]; x_5 – pressure in cylinder chamber two [Pa]; $\omega := x_6$ – pump and motor shaft speed [rad/s]; F_f – internal friction force due the tight sealing [N]; r – reference input (command) [m]; u [V] – control variable. The parameters: $m = 20$ kg – total mass of the piston and the load referred to piston; $f = 10^4$ Ns/m – load viscous damping coefficient; $k = 1\,190\,000$ N/m – load spring gradient; $S = 2 \times 10^{-4}$ m² – piston area; $l = 0.1$ m – half of piston stroke; $V_{D1} = V_{D2} = V = 3.95 \times 10^{-7}$ m³ – dead volumes of the hydraulic lines; $D_p = 1.6925 \times 10^{-7}$ m³/rad – pump displacement; $B = 6 \times 10^8$ Pa – bulk modulus of the oil; $p_a = 207 \times 10^5$ Pa – nominal pressure; $p_r = 5 \times 10^5$ Pa – minimal pressure of the hydraulic system; $k_m = 28.37$ rad/(sV) – motor gain; τ – motor time constant [s]; τ_s – servoactuator time constant [s]; K – controller gain [V/m]; $C_{ec} = 1.9 \times 10^{-13}$ m³/(Pa×s) – external leakage coefficient; $C_{ip} = 2 \times 10^{-13}$ m³/(Pa×s) – internal leakage coefficient; $\sigma_0 = 2 \times 10^4$ N/m – stiffness coefficient; $\sigma_1 = 3 \times 10^2$ Ns/m – damping coefficient; $f_v = 60$ Ns/m – viscous friction coefficient; $v_s = 0.1$ m/s – Stribeck velocity; $F_c = 100$ N – Coulomb friction; $F_s = 120$ N – static friction.

Artificial intelligence based approach in the treatment of control problems concerns in principle an input-output behavioral philosophy of solution. In fact, herein *the mathematical model (1) will serve only as illustration of applying this strategy. In the case of experiment, the mathematical model is naturally substituted by the physical system.*

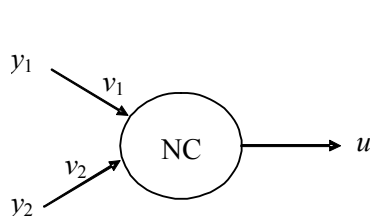


Fig. 2 – Perceptron type neurocompensator.

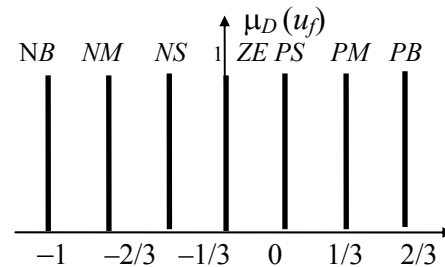


Fig. 3 – Singleton membership function.

The neuro-fuzzy control strategy adopted for the position control of the system is composed of two components: a neuro-control and a fuzzy logic control supervising the neuro-control to counteract the saturation. As neuro-control, a unilayered perceptron is used (Fig. 2)

$$u := u_n = v_1 y_1 + v_2 y_2 =: v_1 (r - z) + v_2 \dot{z}, \quad (2)$$

where $r(t)$ is reference input (command) and $z := x_1$. From the system behavior view point, the input is u_n and the output is $\mathbf{y} = (y_1, y_2)$. From neuro-control training viewpoint, the system performance is assessed by the *cost function*, a criterion supposing a trade-off between the first input y_1 – tracking error, the second input component y_2 and the control u

$$J = \frac{1}{2n} \sum_{i=1}^n (q_1 y_1^2(i) + y_2^2(i) + q_2 u_n^2(i)) := \frac{1}{2n} \sum_{i=1}^n J(i). \quad (3)$$

The weighting vector $\mathbf{v} = [v_1 \ v_2]^T$ is updated online by the gradient descent learning method to reduce the cost J . Consequently, the update is given by the expression

$$\mathbf{v}(n+1) = \mathbf{v}(n) + \Delta \mathbf{v}(n), \Delta \mathbf{v}(n) := -\text{diag}(\delta_1, \delta_2) \frac{\partial J}{\partial \mathbf{v}(n)} = \text{diag}(\delta_1, \delta_2) \sum_{i=n-N}^n \left(\frac{\partial J(i)}{\partial \mathbf{y}(i)} \frac{\partial \mathbf{y}(i)}{\partial u(i)} + \frac{\partial J(i)}{\partial u(i)} \right) \frac{\partial u(i)}{\partial \mathbf{v}(i)}, \quad (4)$$

where the matrix $\text{diag}(\delta_1, \delta_2)$ introduces the learning scale vector, $\Delta \mathbf{v}(n)$ is the weight vector update and N marks a back memory (of N time steps). The derivatives in (4) require only input-output information about the system. $\partial \mathbf{y}(i) / \partial u(i)$ is online approximated by the relationship

$$(\mathbf{y}(i) - \mathbf{y}(i-1)) / (u(i) - u(i-1)). \quad (5)$$

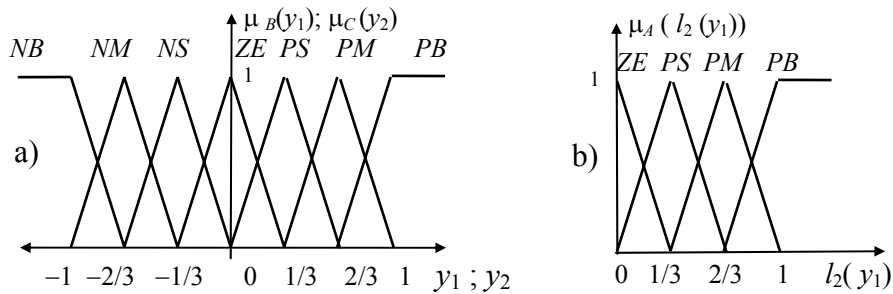


Fig. 4 – Membership functions for: a) scaled input variables y_1, y_2 and b) $l_2(y_1)$.

To counteract the risk of neuro-control saturation and achieve the goal of reinforcement learning system, a Fuzzy Supervised Neuro-control (FSNC) was proposed in [11]. FSNC switches to a Mamdani type fuzzy logic control when the just described neuro-control saturated.

Further on, the three standard components of the fuzzy control: fuzzyfier, fuzzy reasoning, and defuzzyfier, will be succinctly exemplified. The used *fuzzyfier* component converts the crisp input signals

$$l_2(y_{1k}): = \sqrt{\sum_{j=k-2}^k y_{1j}^2}, \quad y_{1k}, \quad y_{2k}, \quad k = 1, 2, \dots \quad (6)$$

into their relevant fuzzy variables (or, equivalently, membership functions) using the following set of linguistic terms: zero (ZE), positive or negative small (PS, NS), positive or negative medium (PM, NM), positive or negative big (PB, NB) (for the sake of simplicity, triangular and singleton type membership functions are chosen, see Figs. 3, 4). l_2 is a norm which computes, over a sliding window with a length of 3 samples, the maximum variation of the tracking error. The insertion of this crisp signal in the fuzzyfier will result in a reduction of fuzzy control switches due to the effects of spurious noise signals.

The strategy of *fuzzy reasoning* construction embodies herein the idea of a (direct) *proportion between the error signal y_1 and the required fuzzy control u_f* . Thus, the fuzzy reasoning engine totals a number of

$n = 4 \times 7 \times 7$ IF..., THEN... rules, that is the number of the elements of the Cartesian product $A \times B \times C$, $A := \{ZE; PS; PM; PB\}$, $B = C := \{NB; NM; NS; ZE; PS; PM; PB\}$. These sets are associated with the sets of linguistic terms chosen to define the membership functions for the fuzzy variables $l_2(y_1)$, y_1 and, respectively, y_2 . Consequently, the succession of the n rules is the following: 1) IF $l_2(y_1)$ is ZE and y_2 is PB and y_1 is PB, THEN u_f is PB; 2) IF $l_2(y_1)$ is ZE and y_2 is PB and y_1 is PM, THEN u_f is PM; ... 7) IF $l_2(y_1)$ is ZE and y_2 is PB and y_1 is NB, THEN u_f is NB; 8) IF $l_2(y_1)$ is ZE and y_2 is PM and y_1 is PB, THEN u_f is PB; ... 196) IF $l_2(y_1)$ is PB and y_2 is NB and y_1 is NB, THEN u_f is NB.

Let T be the discrete sampling time. Consider the three scaled input crisp variables $l_2(y_{1k})$, y_{1k} and y_{2k} , at each time step $t_k = kT$ ($k = 1, 2, \dots$). Taking into account the two ordinates corresponding in Figs. 3, 4 to each of the three crisp variables, a number of $M \leq 2^3$ combinations of three ordinates must be investigated. Having in mind these combinations, a number of M IF..., THEN... rules will operate in the form

$$\text{IF } y_{1k} \text{ is } B_i \text{ and } y_{2k} \text{ is } C_i \text{ and } l_2(y_{1k}) \text{ is } A_i, \text{ THEN } u_{fk} \text{ is } D_i, \quad i = 1, 2, \dots, M \quad (7)$$

(A_i, B_i, C_i, D_i are linguistic terms belonging to the sets A, B, C, D and $D = B = C$, see Figs. 3, 4). The *defuzzifier* concerns just the transforming of these rules into a mathematical formula giving the output control variable u_f . In terms of fuzzy logic, each rule of (10) defines a fuzzy set $A_i \times B_i \times C_i \times D_i$ in the input-output Cartesian product space $R^+ \times R^3$, whose membership function can be defined in the manner

$$\mu_{u_i} = \min \left[\mu_{B_i}(y_{1k}), \mu_{C_i}(y_{2k}), \mu_{A_i}(l_2(y_{1k})), \mu_{D_i}(u) \right], \quad i = 1, \dots, M \quad (k = 1, 2, \dots) \quad (8)$$

For simplicity, the singleton-type membership function $\mu_D(u)$ of control variable has been preferred; in this case, $\mu_{D_i}(u)$ will be replaced by u_i^0 , the singleton abscissa. Therefore, using 1) the singleton fuzzyfier for u_f , 2) the center-average type defuzzifier, and 3) the min inference, the M IF..., THEN... rules can be transformed, at each time step $k\tau$, into a formula giving the crisp control u_f [13]

$$u_f = \frac{\sum_{i=1}^M \mu_{u_i} u_i^0}{\sum_{i=1}^M \mu_{u_i}} \quad (9)$$

The FSNC operates as fuzzy logic control u_f in the case when neuro-control u_n saturated, or so called l_2 -norm of tracking error y_1 increased. In the case of fuzzy control operating, the fuzzy neuro-control u_n is concomitantly updated in the context of the real acting fuzzy control u_f . To obtain the rigor and accuracy of regulated process tracking, fuzzy logic control switches on neuro-control whenever readjusted neuro-control u_n is not saturated and scaled norm $l_2(y_1)$ is smaller than a chosen value $l_{2,\min}$. At time t_s , when the switching from fuzzy logic control to neuro-control occurs, the readjusted weighting vector v_r will be derived by considering a scale factor u_f/u_n [14]

$$v_{1r} = (u_f - v_2 y_2) u_f / (u_n y_1), \quad v_{2r} = v_2 u_f / u_n \quad (10)$$

The aforementioned control was brought to the proof in numerical simulations reported in [4–6]. In accordance with simulation studies, in [5] it is proved that: a) the nonconventional neurofuzzy control, as compared with a proportional control, improves the transients of SHA dynamics, mainly in the case of sinusoidal references: thus, a better tracking, meaning smaller attenuation and dephasage, are achieved; b) the neurofuzzy control is proved to ensure a more robust control of SHA than the classical proportional control. Moreover, as it can be seen in next Section, the theoretical basic performance parameter, the time constant, is very close to the experimental one.

3. EXPERIMENTAL RESULTS

To test the proposed neuro-fuzzy control strategy and study fundamental problems associated with the control of hydrostatic HSA systems, the cylinder doublet – each part having simple action – is supplied with

hydraulic oil by a fixed displacement, bidirectional Haldex Hydraulics HX G2204C1A300N00 gear pump. The transmission of the fluid power is obtained by very stiffly coupling the pump to the hydraulic cylinder. The pump is driven by an AC Anaheim BLW235S-36V-4000 electric motor. A planetary gearbox with 3:1 gear ratio is a part of electric motor. The main data of the pump: pump displacement – $1.07 \text{ cm}^3/\text{rot}$; nominal pressure – 207 bar; pump (and motor shaft) maximal speed (rad/s) – 3 600 rpm; maximal flow – 3.86 l/min. The main data of the electric motor: peak torque – 1.3 Nm; rated power – 180 W; rated speed 4 000 rpm; mass – 1.4 kg; peak current – 22.5 A; rated voltage – 36 V; control maximal voltage – $\pm 5 \text{ V}$. A view of the motor-pump-hydraulic cylinder components of the system on the test rig is shown in Fig. 6.



Fig. 6 – View of the test rig for the hydrostatic actuator.

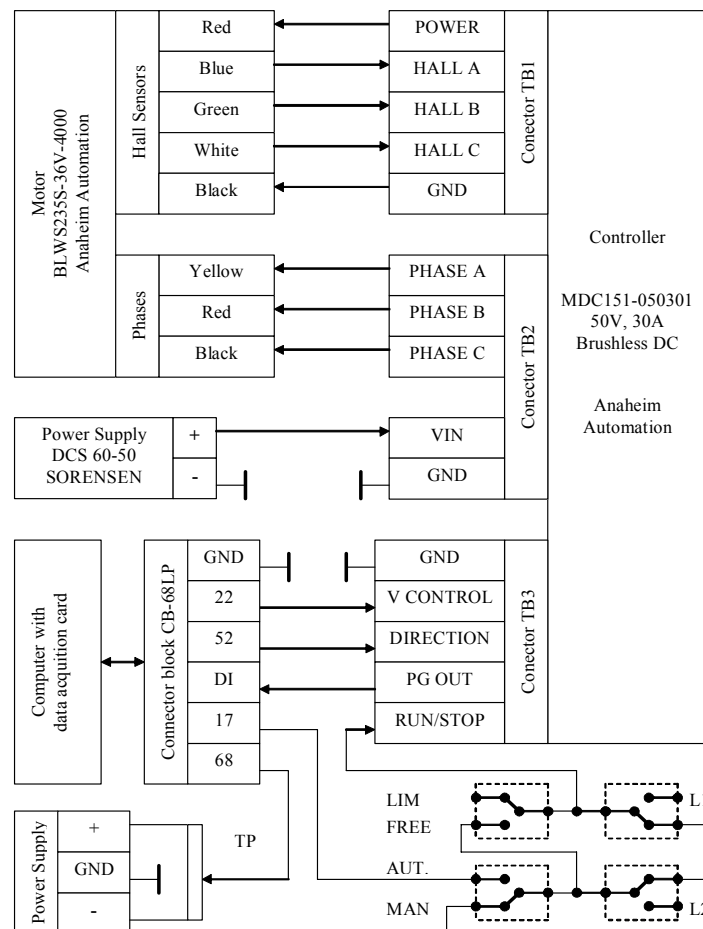


Fig. 7 – Electrical connection diagram.

The experimental set up is presented in Fig. 7. The switches labeled L1 and L2 are used to stop the electrical motor at a stroke about than half of maximum stroke of the piston, as a measure of safety. The switch with positions labeled LIM (limited) and FREE is used to enable this protection on the LIM position. The other switch is used to select the motor command, MAN (manually) or AUT (automatically).

Conclusive experimental recordings are presented in Figs. 8, 9, which show time responses to sinusoidal combination, respectively, step references. Implementation of neuro-fuzzy algorithm described in Section 2 was performed using LabView programming language. The initial values of weighting vector v has proven to have a certain, but not decisive importance. As it can be seen from Fig. 9, a value of the actual servoactuator time constant $\tau_s = 0.0824$ s is obtained. This value is confirmed by a theoretical evaluation. Indeed, let us consider the paradigmatic structure of the control (compare with (2))

$$u = K(r - z). \quad (11)$$

A reduced mathematical model derived from (1) is

$$\begin{aligned} m\ddot{z} + \hat{f}\dot{z} + kz &= Sp, \quad p := x_4 - x_5, \\ \frac{V}{B}\dot{x}_4 &= D_p x_6 - S\dot{z}, \quad \frac{V}{B}\dot{x}_4 = -D_p x_5 + S\dot{z}, \quad \tau\dot{x}_6 + x_6 = k_m u. \end{aligned} \quad (12)$$

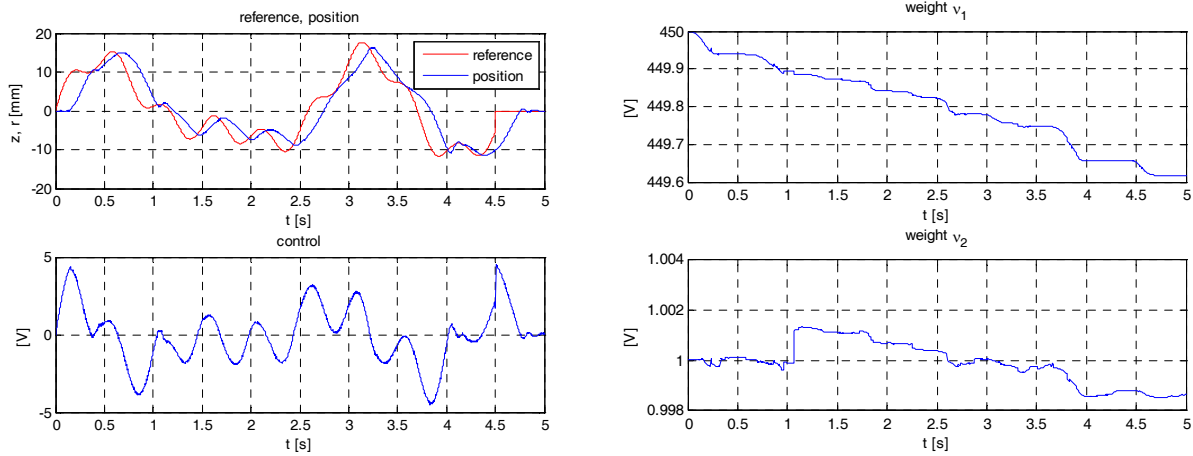


Fig. 8 – Experimental recording, neuro-fuzzy control, sinusoidal signals combination reference. Time histories for reference r , position z and control u variables (left) and weighting vector v (right).

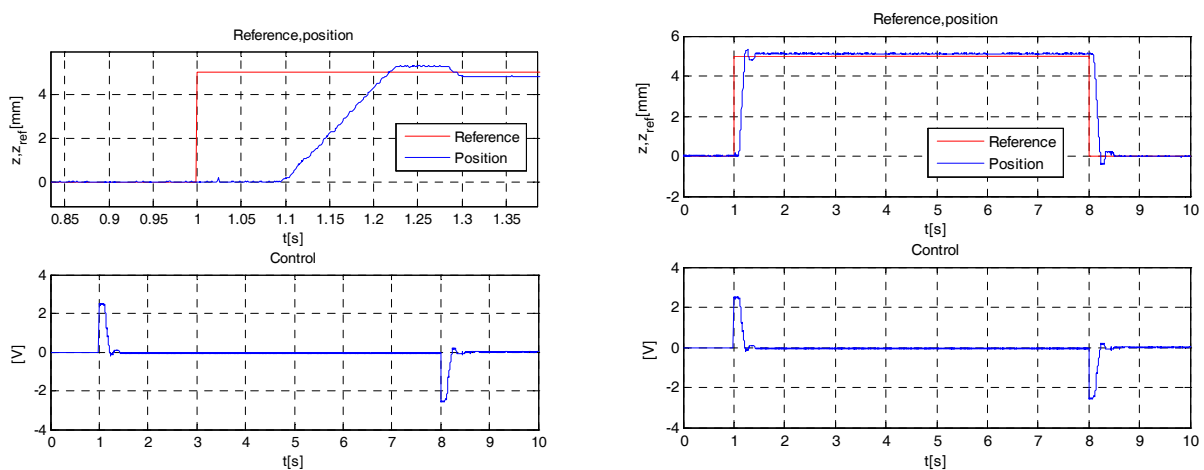


Fig. 9 – Experimental recording: neuro-fuzzy control, step reference signal. The result: actual servoactuator time constant $\tau_s = .0824$ s (delay ignored!). Time histories for reference r , position z and control u variables (left) and b) zoom on left figure.

From (11)–(12), the transfer function $r \rightarrow z$ can be written as

$$\left\{ (\tau s + 1) \left[ms^3 + fs^2 + \left(k + \frac{2S^2B}{V} \right) s \right] + \frac{2SBD_p k_m K}{V} \right\} z = \frac{2SBD_p k_m K}{V} r. \quad (13)$$

The system can be expressed as an order one system in the manner

$$(a_0 s + a_1) z = b_0 r, \quad (14)$$

so we have the time constant

$$\tau_s = \frac{a_0}{a_1} = \frac{\frac{k + 2S^2B}{V}}{\frac{2SBD_p k_m K}{V}} = \frac{kV + 2S^2B}{2SBD_p k_m K} \quad (15)$$

or, taking into account the value $k \cong 0$ in experiment,

$$\tau_s \cong \frac{S}{D_p k_m K}. \quad (15')$$

To determine motor speed-control voltage gain k_m , the measurement shown in Fig. 10 was performed, with 1V control voltage in loaded regime; the found time constant is $\tau = 0.265$ s. Based on the equation $\tau \dot{x}_6 + x_6 = k_m u$, we have

$$0.265 \frac{\theta_1 - \theta_0}{\Delta t} + \theta_0 = k_m, \quad 0.265 \frac{300 - 0}{0.0978} + 0 = k_m, \quad k_m = 85.12 \text{ rad}/(\text{sV})$$

but a speed reduction factor 1/3 from motor to pump is involved, thus

$$k_m = 85.12/3 \text{ rad}/(\text{sV}) = 28.37 \text{ rad}/(\text{sV}).$$

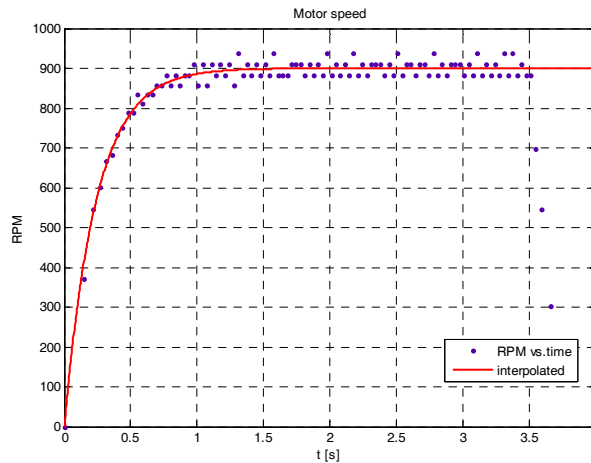


Fig. 10 – Measuring motor time constant τ and angular speed-control voltage gain k_m in loaded regime, 1 V control input.

Substituting in (15') the cylinder-pump-motor main data and the controller gain K

$$S = 2 \times 10^{-4} \text{ m}^2, \quad D_p = 1.7 \times 10^{-7} \text{ m}^3/\text{rad}, \quad k_m = 28.37 \text{ rad}/(\text{sV}), \quad K = 450 \frac{\text{V}}{\text{m}}$$

gives $\tau_s \cong 0.09$ s that is a value close to the experimental value $\tau_s \cong 0.0824$ s. The size of controller gain K is in fact provided as the value of v_1 weight in Fig. 8, where v_2 is relatively negligible.

5. CONCLUSIONS

The studies and experimental results in the literature show that the neuro-fuzzy control not only extends the system bandwidth, but also provides excellent control performance [10–12, 14], as compared with various classical control strategies in hydraulic servo position systems [15–19].

Considering previous researches of the authors [11,14], the main conclusion of the paper concerns the remarkable fact that neuro-fuzzy control algorithm ensured well dynamical behavior of the hydrostatic servoactuator. Let note the most meaningful feature of this proposed controller: because is in fact a free model strategy, this methodology ensures a reduced design complexity and provides antisaturating and antichattering properties of the controlling system [9], thus favourising its robustness.

ACKNOWLEDGEMENTS

The authors gratefully acknowledge the financial support of the National Authority for Scientific Research –ANCS, UEFISCSU, through PN-II research project code ID 1391/2008. The authors would like, also, to thank the colleague eng. Vladimir Berar for his precious assistance in the experimental tests.

REFERENCES

1. *** Cost-Effective Small Aircraft-CESAR, Contract 30888, FP6 Integrated Project, 2006.
2. PASTRAKULJIC, V., *Design and modeling of a new electrohydraulic actuator*, MS Thesis, University of Toronto, 1995.
3. HABIBI, S., GOLDENBERG, A., *Design of a new high performance electrohydraulic actuator*, IEEE/ASME Transaction on Mechatronics, **5**, 2, pp. 158–164, 2000.
4. TOADER, A., URSU, I., *Backstepping control synthesis for hydrostatic type flight controls electrohydraulic actuators*, Annals of the University of Craiova, Series Automation, Computers, Electronics and Mechatronics, **4** (31), 1, 122–127, 2007.
5. URSU, I., G. TECUCEANU, URSU, F., TOADER, A., *Nonlinear control synthesis for hydrostatic type flight controls electrohydraulic actuators*, Proceedings of the International Conference in Aerospace Actuation Systems and Components, Toulouse, June 13–15, pp. 189–194, 2007.
6. *** PN-II research project Hydrostatic Servoactuator for Airplanes-SAHA, INCAS Contract 81 036/2007 with Romanian Ministry of Education and Research, National Authority for Scientific and Technological Research (former CNMP).
7. BALEA, S., HALANAY, A., URSU, I., *Coordinate transformations and stabilization of some switched control systems with application to hydrostatic electrohydraulic servoactuators*, Control Engineering and Applied Informatics, **12**, 3, pp. 67–72, 2010.
8. HALANAY, A., URSU, I., *Stability analysis of equilibria in a switching nonlinear model of a hydrostatic electrohydraulic actuator*, in: *Mathematical Problems in Engineering Aerospace and Science*, Volume 5, Cambridge Scientific Publishers, 2010, S. Sivasundaram (Ed.)
9. URSU, I., URSU, F., *Active and semiactive control* (in Romanian), Romanian Academy Publishing House, 2002.
10. URSU, I., URSU, F., *New results in control synthesis for electrohydraulic servo*, International Journal of Fluid Power, **5**, 3, November-December, pp. 25–38, 2004.
11. URSU, I., URSU, F., IORGA, L., *Neuro-fuzzy synthesis of flight controls electrohydraulic servo*, Aircraft Engineering and Aerospace Technology, **73**, pp. 465–471, 2001.
12. URSU, I., URSU, F., POPESCU, F., *Backstepping design for controlling electrohydraulic servos*, Journal of The Franklin Institute, **343**, 1, 94–110, 2006.
13. WANG, L.-X., KONG, H., *Combining mathematical model and heuristics into controllers: an adaptive fuzzy control approach*, Proc. of the 33rd IEEE Conference on Decision and Control, Buena Vista, Florida, December 14–16, **4**, pp. 4122–4127, 1994.
14. URSU, I., URSU, F., *Airplane ABS control synthesis using fuzzy logic*, Journal of Intelligent&Fuzzy Systems, **16**, 1, pp. 23–32, 2005.
15. MIHAILOV, M., NIKOLIC, V., ANTIC, D., *Position control of an electro-hydraulic servo system using sliding mode control enhanced by fuzzy PI controller*, FACTA UNIVERSITATIS Series: Mechanical Engineering, **1**, 9, pp. 1217–1230, 2002.
16. VASILIU, N., CALINOIU, C., VASILIU, ION-GUTA, D., *Improving the accuracy of the electrohydraulic servomechanisms by additional feedbacks*, Proceedings of the Romanian Academy, Series A, Mathematics, Physics, Technical Sciences, Information Science, **10**, 3, pp. 277–284, 2009.
17. JELALI, M., KROLL, A., *Hydraulic servo-systems*, 1st ed., Springer, 2002.
18. YAO, B., REEDY, J. T., CHIU, C. T.-C., *Adaptive robust motion control of single rod hydraulic actuators: theory and experiments*, IEEE/ASME Transactions on Mechatronics, **5**, pp. 79–91, 2000.
19. KEMMETMULLER, W., KUGI, A., *Immersion and invariance-based impedance control for electrohydraulic systems*, International Journal of Robust and Nonlinear Control, **20**, 7, pp. 725–844, 2010.

Received January 27, 2011